Journal of Transport Geography 128 (2025) 104383

Contents lists available at ScienceDirect

Journal of Transport Geography

journal homepage: www.elsevier.com/locate/jtrangeo

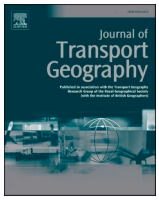

Measuring exposure to extreme heat in public transit systems☆

Luyu Liu [a,*], Xiaojiang Li [b], Rafael H.M. Pereira [c], Xiang Yan [d]

[a] Department of Geosciences, Auburn University, AL, USA
[b] Weitzman School of Design, University of Pennsylvania, PA, USA
[c] Institute for Applied Economic Research, Brasília, Brazil
[d] Department of Civil and Coastal Engineering, University of Florida, Florida, USA

ARTICLE INFO

Keywords:
Heat exposure
Public transit
Urban heat island effect
Microclimate simulation
Thermal comfort
Transit heat exposure index

ABSTRACT

Public transit users are among the most vulnerable to extreme heat due to the urban heat island effect and longer outdoor exposure. However, few studies have provided detailed measurement of transit riders' heat exposure and discussed the resilience of transit systems in responses to heat exposure. Using 1 m-by-1 m microclimate simulations and transport network analysis, this paper introduces the *Transit Heat Exposure Index* (THEI) to gauge high-fidelity heat exposure for transit riders. A case study of THEI's application in Miami, one of the hottest US cities, shows that downtown Miami has lower heat exposure due to better transit access, despite higher local feels-like temperature. Walking is the primary source of heat compared to waiting, and a few streets and stops contribute most exposure. The methodology developed in this study provides a valuable tool to enhance transit resilience to heat and develop effective mitigation strategies.

1. Introduction

Extreme heat events present significant risks to public health, infrastructure security, and the environment. Extreme heat can cause heat exhaustion and heat stroke, which exacerbates preexisting conditions and increase mortality (Dong et al., 2020). Exposure and heat-related incidents are projected to become more frequent and severe in urban environments due to climate change (Klein and Anderegg, 2021).

Transportation is a major source of heat exposure, especially for public transit riders (Fraser and Chester, 2017). Compared with other motorized modes of transportation, public transit riders experience more extreme heat exposure due to long exposure time when walking and waiting and urban heat island effect (Hsu et al., 2021; L. Liu et al., 2022). The lack of tree canopies and shades can further exacerbate the heat exposure (X. Li, 2021). As socially disadvantaged and marginalized groups tend to rely on public transit services and lack reliable transportation alternatives, transit heat exposure is also a major equity issue to be addressed (Dzyuban et al., 2021). Therefore, extreme heat exposure has major impacts on the resilience of public transit systems.

The existing studies on transit heat exposure have limitations (Gu et al., 2024; Huang et al., 2024; R. Li et al., 2023). First, most prior studies do not consider travel behavior (e.g., travel time and route choice) as a factor in the calculation of heat exposure (Kuras et al., 2017; Nazarian and Lee, 2021; Park and Kwan, 2017), even though exposure time can be as important as the local temperature. Second, despite abundant studies on the community-level thermal comfort and urban heat island effect, there is a lack of high-resolution, individual-level heat exposure analysis at 1 m level (Kuras et al., 2015). Finally, to our best knowledge, no prior studies investigated the primary source of heat exposure in transit trips.

Considering the research gaps discussed above, this paper introduces a novel methodology to measure high-resolution heat exposure for public transit riders with a case study of Miami, Florida. We use high-resolution meteorological data, tree canopy, and building LiDAR data to calculate a 1 m-by-1 m feels-like temperature map. We also use General Transit Feed Specification (GTFS) data to generate high-fidelity travel itinerary between all census block groups. Based on these high-resolution datasets, we create a new transit-based heat exposure measure – Transit Heat Exposure Index (THEI) – to measure the high-resolution heat exposure during public transit trips. We further conduct spatiotemporal analyses and examine the sources of heat exposure in different scales. Based on these empirical results, we discuss the implications of extreme heat exposure on the resilience of public transit systems.

☆ This article is part of a Special issue entitled: 'Transport Resilience' published in Journal of Transport Geography.

* Corresponding author at: 2046J Haley Center, Auburn, AL 36849, USA.
E-mail address: luyuliu@auburn.edu (L. Liu).

https://doi.org/10.1016/j.jtrangeo.2025.104383
Received 23 November 2024; Received in revised form 30 March 2025; Accepted 29 July 2025
Available online 11 August 2025

The paper is structured as follows. We first review the prior literature about the measurement of extreme heat and public transit in section 2. We then introduce our data and method in section 3. We then present our results and discussion in section 4. We finally conclude the paper with some high-level insights to provide useful guidance for future research and practical planning.

2. Background

This section reviews the literature on extreme heat exposure and public transit, organized into three distinct subsections: the measurement of extreme heat exposure, the implications of the built environment for heat exposure, and heat exposure in public transit systems.

2.1. Measuring extreme heat exposure in urban areas

The measurement of extreme heat exposure has evolved significantly in recent decades, reflecting advancements in technology and a growing understanding of heat's impact on both the environment and human health (Deschenes, 2014; Wong et al., 2013). In some early studies, basic thermometry was the primary method for measuring ambient temperatures (Saaroni et al., 2000). However, these methods were limited in scope, focusing solely on ambient temperature without considering other environmental factors or human physiological responses to heat (R. Li et al., 2023). Technological advancements such as satellite imaging have enabled large-scale monitoring of surface temperatures and the identification of heatwaves, significantly enhancing our ability to track and analyze global heat exposure trends (Hu et al., 2023). Additionally, the field of biometeorology introduced human-centric measures, integrating human physiological responses to heat into the assessment of heat exposure (Kuras et al., 2017). This led to the development of thermal comfort models like the Predicted Mean Vote (PMV) (Yau and Chew, 2014) and Standard Effective Temperature (SET) (Iseki and Tingstrom, 2014). More recent progresses include Mean Radiant Temperature (MRT) (Vanos et al., 2021) and Universal Thermal Climate Index (UTCI) (Romaszko et al., 2022), which marked a shift towards a more nuanced understanding of heat exposure, considering not just environmental parameters but also their direct impact on human health and well-being.

2.2. Heat exposure and built environment

Built environment has major impacts on human exposure to extreme heat, especially for urban dwellers (X. Li, 2021; Nazarian and Lee, 2021). One of the central themes in this body of research is the urban heat island (UHI) effect. The domain primarily study urban areas that experience higher temperatures than their rural counterparts nearby (Hsu et al., 2021; Yin et al., 2023).

UHI is driven by three main factors: land cover and albedo, urban tree canopy, and buildings (Chen et al., 2023; Lu et al., 2021). Urban areas often consist of impervious surfaces such as concrete and asphalt, which have low albedo, causing them to absorb and retain heat (Y. Liu et al., 2024; Nwakaire et al., 2020). This contributes to increased temperatures within cities. Meanwhile, tree canopy and buildings can provide shades that reduce heat, while trees can have more cooling effects via evaporation (Cheung, 2018; Zhang et al., 2022). Previous research has shown that trees can lead to average daytime cooling impacts of 0.6 °C for air temperature and 2.5 °C for feels-like temperature, surpassing those of concrete shelters, which recorded 0.2 °C for air temperature and 2.0 °C for feels-like temperature, respectively (Cheung, 2018).

2.3. Heat exposure and public transit

Previous studies have examined how individuals can be exposed to varying levels of heat while they move across cities, focusing on groups such as outdoor joggers and food delivery riders (X. Li and Wang, 2021a; Y. Liu et al., 2024). So far, very few papers have investigated the heat exposure of public transit riders. Karner et al. (2015) was among the first to discuss the heat exposure experienced by users of public transit as well as other non-motorized travel modes, including walking and biking. Using simulated trips and 1 km resolution air temperature data, they revealed that disadvantaged groups are disproportionately affected by extreme heat. Fraser et al. (2017) estimated heat exposure from walking to and waiting at bus stops by using shortest distance to the nearest bus stop and bus schedules. The paper found that transit users from low-density and low-connectivity areas had higher expected exposure due to longer walking distances and waiting times. Moreover, Dzyuban et al. (2021) surveyed public transit riders about their perceptions of heat and behavior changes to cope with heat in Phoenix, Arizona. More recently, Fan et al. (2024) introduced a new framework to measure cumulative exposure to extreme temperatures during transit trips. They used 30 m-by-30 m temperature data and GTFS data in Atlanta, Georgia with a regional onboard transit survey to calculate the dynamics in transit trips and cumulative exposure for transit riders in 2019.

3. Methods

We introduce our proposed method in this section. We first present our case study and data. We then describe two major methodological steps of calculating high-resolution thermal comfort data and detailed itineraries. Next, we introduce the definition of *Transit Heat Exposure Index (THEI)* and the details of the analyses.

3.1. Data

In this study, we utilized diverse datasets from various sources to measure thermal comfort and travel behavior of public transit riders as shown in Table 1.

3.1.1. Transit network data

We used the General Transit Feed Specification (GTFS) data, the de facto data standard for public transit schedule timetable (Google Developers, 2020). The GTFS data for Miami-Dade County Transit are captured near August 1st, 2023 from the Transitfeeds.com (OpenMobilityData, 2023), when the average temperature was highest in 2023. We use the OpenStreetMap network data in September 2023 as the data source of sidewalk network.

Table 1
Data summary of the THEI.

Data type	Data name	Time period	Source
Transportation data	GTFS schedule data	August 2023	OpenMobilityData (2023)
	OSM road network	September 2023	Geofabrik (2023)
	LODES travel survey	2021	US Census Bureau Center for Economic Studies (2023)
Meteorological data	Air temperature data	August 2020	NREL (2024)
	Global horizontal radiation		
	Direct radiation		
	Diffuse radiation		
	Relative humidity		
Built environment data	Building footprint	2014–2023	Microsoft (2024)
	LiDAR cloud point	2004–2023	U.S Geological Survey (2023)
	Multispectral NAIP imageries	2023	National Agriculture Imagery Program (2023)

3.1.2. Meteorological data

We collected the meteorological data, including average air temperature, global horizontal radiation, direct radiation, diffuse radiation, and average relative humidity data, from the NREL data portal for the city of Miami as constants (NREL, 2024). All data were collected at the latest available timepoint, i.e., August 2020.

3.1.3. Built environment data

We used the building footprint map from Microsoft building footprint database (Microsoft, 2018/2024). We also used the most recent high-resolution LiDAR cloud point datasets from United States Geological Survey (U.S Geological Survey, 2023) and generated 1 m-by-1 m digital surface model (DSM). We then used the 1 m-by-1 m multispectral NAIP imageries and generated the tree canopy cover maps using the thresholding method on the normalized difference vegetation index (NDVI) (National Agriculture Imagery Program, 2023). We then refined the tree canopy maps based on the generated DSM, and we removed those pixels lower than 2 m, since the tree shades lower than 2 m is negligible. The building footprint map and the generated tree canopy map were then overlayed on the DSMs to generate the building height model and tree canopy height model for the study area.

Our case study focuses on the city of Miami, Florida, USA. Florida is one of the most vulnerable areas to heat exposure and heat-related mortality in the United States (Keellings and Waylen, 2014), and Miami is among the hottest city in the US with an average annual temperature of 26 °C from 2009 to 2021 (World Weather Online, 2024); The hottest month ever recorded was July 2023, when the temperature was higher than 37 °C for 46 consecutive days in Miami (Crowley, 2023). Heat-related mortality in Miami was also reported to be much higher than northern cities in the US (Curriero et al., 2002), with the duration and frequency of the extreme heat events expected to be much higher due to climate change (McAllister et al., 2022). Furthermore, Florida is the third most populous state in the US with over 20 % of its population older than 65 years old, who are more susceptible to heat exposure and heat-related illnesses (US Census Bureau, 2020).

3.2. Feels-like temperature calculation

The mean radiant temperature (T_{mrt}) is the net shortwave and longwave radiation to which human body exposed from the surrounding environment and the T_{mrt} is the most significant meteorological input parameter for the human energy balance especially during clear and calm summer days (Mayer and Höppe, 1987). Per the Stefan-Boltzmann law, T_{mrt} is defined as,

$$T_{mrt} = \sqrt[4]{R/\varepsilon_p \sigma} - 273.15 \quad (1)$$

where σ is the Stefan-Boltzmann constant and ε_p is the emissivity of the

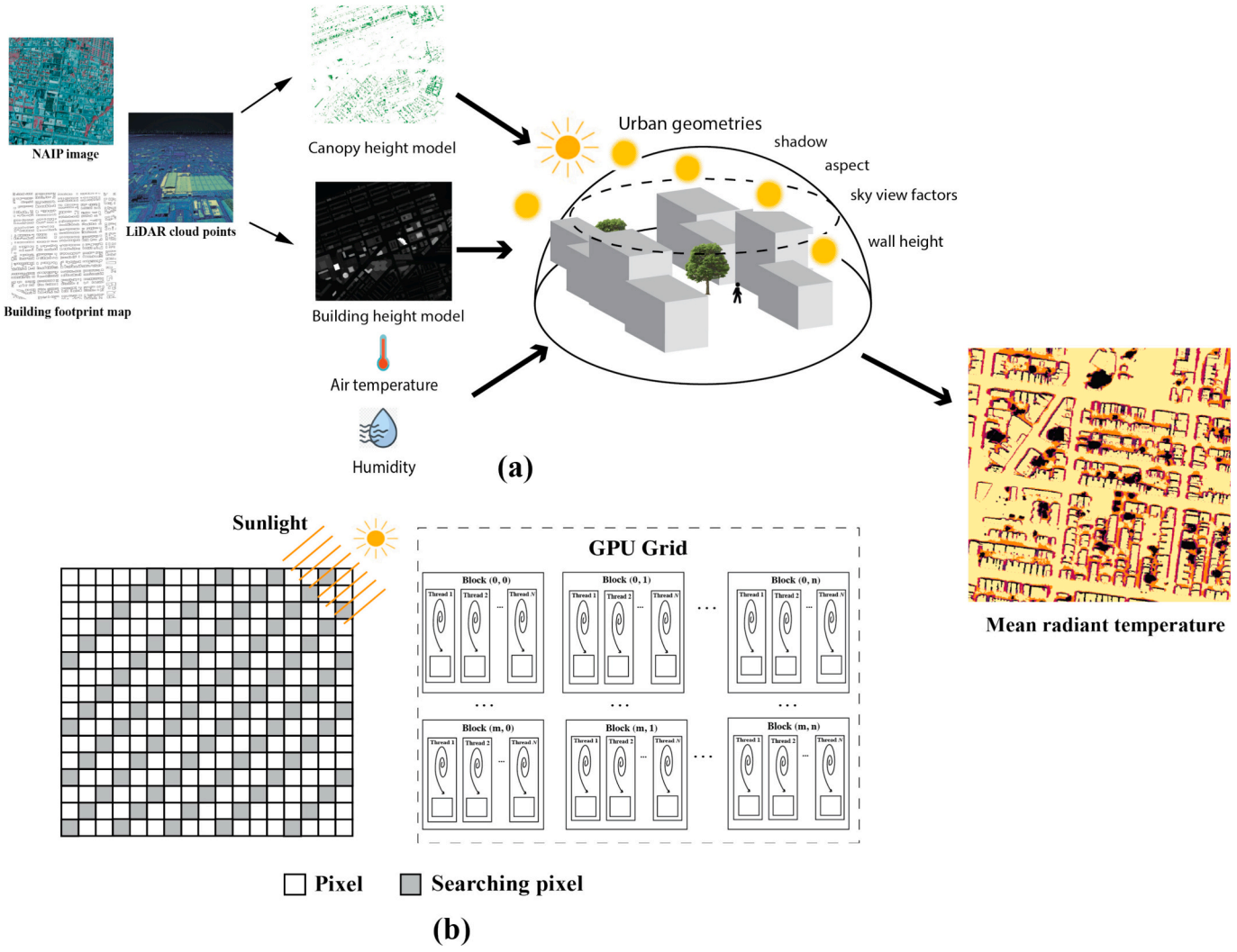

Fig. 1. The calculation of the T_{mrt} with the SOLWEIG model based on tree canopy height model, building height model, and meteorological data using the GPU-accelerated algorithm, (a) the SOLWEIG model for computing the mean radiant temperature, (b) the GPU structure.

human body with the standard value of 0.97. R represents total radiation exposure as the sum of short and long wave radiation from above, below, and the four cardinal directions, which can be calculated as,

$$R = \xi_k \sum_1^6 K_i F_i + \varepsilon_p \sum_1^6 L_i F_i \quad (2)$$

where K_i is the shortwave radiation component from west, east, north, south, top, and bottom, L_i is the longwave radiation, F_i is the angular factor between an individual and their surrounding environment, ξ_k is the absorption coefficient for shortwave radiation with a standard value of 0.7. We used the GPU-accelerated Solar and LongWave Environmental Irradiance Geometry model (SOLWEIG) (X. Li and Wang, 2021b) to calculate the T_{mrt} with the meteorological and built environment data (Fig. 1). We chose to calculate the temperature with 1 m-by-1 m resolution. This high-resolution analysis is to match the detailed network simulation generated from transport network analysis at the meter and second level. The heat exposure data must also match this level of granularity to accurately calculate high-resolution exposure for each trip. For example, sidewalk widths are usually 1–2 m wide, and the area of a single tree canopy is also at a similar scale. Therefore, feels-like temperature can be very different within even several meters. Using lower-resolution heat exposure data could introduce bias, as it may overlook these fine-scale variations that significantly impact exposure calculations.

3.3. Transport network analysis

We conducted public transit network analysis to generate the detailed itineraries of transit trips in the form of origin-destination matrix. We first chose the centroids of census block groups as the origins and destination to simulate the door-to-door travels, because census block groups are the smallest geographic units with the most up-to-updated LODES data, which can serve as the weight when aggregating the heat exposure measure.

We then calculated the shortest path between each OD pair. We used an open-source solution – *r5r* – an R package that calculates rapid realistic routing for multimodal transportation networks (Pereira et al., 2021). We utilized r5r's *detailed itinerary* function, which outputs the detailed trip information between origin-destination pairs, including first/last-mile walking time, waiting time, in-vehicle time, and geometry for each trip. We set the maximum walk time as 30 min, the maximum trip duration as 60 min, walk speed as 1 m/s, and maximum rides as 3 rides. We also calculated the average travel time from August 1st to August 7th, 2023. We imported the large amount of CSV files generated by the package and synthesized the data into organized records in a single collection in a MongoDB database.

3.4. Exposure measurement

We introduce the Transit Heat Exposure Index (THEI), a new measure that considers both temperature and temporal factors. We adopt a *total degree-second* approach, i.e., the sum product of feels-like temperature and exposure time, to construct the measurement similar to Karner et al. (2015) and Ahmed et al. (2024). Compared with air or ground temperature, Mean Radiant Temperature (MRT) can better capture personal thermal comfort experience; MRT is also more suitable in the sense of thermodynamics as MRT is an additive measure of the net exchange of radiant energy between the human body and the surrounding environment. We define the heat exposure from census block group i to j as:

$$h_{ij} = h_{ij}^t + h_{ij}^w + h_{ij}^v = \sum_k t_{ijk}^t \cdot T_{ijk}^t + \sum_l t_{ijl}^w \cdot T_{ijl}^w \quad (3)$$

The total heat exposure can be decomposed into three sections based on the environment the users are experiencing in a typical transit trip: h_{ij}^t, i.e., walking along a road link, h_{ij}^w, i.e., waiting at a bus stop, and h_{ij}^v, i.e., riding in a vehicle.

- **Walking.** t_{ijk}^t is the walking travel time along road segment k when travelling from origin i to destination j, including first-mile, last-mile, and transfer, and T_{ijk}^t is the MRT in the corresponding location. In practice, we calculate the cumulative MRT in each road link by overlaying the generated MRT raster against the road network using the method *ZonalStatisticsAsTable* in ArcGIS Pro.
- **Waiting.** Similarly, t_{ijl}^w is the waiting time at stop l when travelling from origin i to destination j, and T_{ijl}^w is the feels-like temperature at stop l.
- **In-vehicle.** In this study, we assume that users do not suffer from heat exposure in the vehicles, since all buses in Miami have air conditioning. However, it is also important to note that this assumption only hold for the context of United States. For many cities in the Global South, heat exposure when riding is an equally important issue and might be aggravated due to passenger crowding (Arbex and Cunha, 2020).

Fig. 2 shows the methodological structure of THEI as discussed above.

3.5. Analysis

With the heat exposure measured for each individual OD pair, we performed aggregations at various analytical levels to better understand the spatiotemporal patterns.

3.5.1. Total transit heat exposure index (Total THEI)

We introduce *total THEI to* capture the sum of the potential heat exposure that would have been experienced by transit riders travelling between all origin-destination pairs weighted by the number of trips between each OD pair. As such, total THEI consists of two components: one is the *potential* exposure of each trip, and the other is the number of passengers taking those trips. When taking the trip origins as a reference, total THEI is defined as

$$H_i^o = \sum_j w_{ij} \cdot h_{ij} \quad (4)$$

Where H_i^o is the origin-based total exposure for the origin i. h_{ij} is the heat exposure for the OD link. Note that we aggregate the OD links to their origin here, which measures the total exposure experienced by riders departing from the census block group i when accessing all other destinations. w_{ij} is a weight to aggregate the exposure of different OD pairs, which can be based on actual ridership, potential demand, or local and destination demographics. We used the most recent commuter flows in 2021 from Longitudinal Employer-Household Dynamics (LODES) data as a yearly proxy for potential trips across OD pairs. Ridership data of higher resolution and quality can also be used as the weight, such as mobile device GPS data or smart card data; however, it is noteworthy that aggregated ridership data, such as Automatic Passenger Counter (APC) data, cannot be used due to the lack of OD flow information.

We also aggregated the OD links to their destination and produced a destination-based heat exposure, which measures the exposure experienced by all riders that travel to the census block group j. It is defined as

$$H_j^D = \sum_i w_{ij} \cdot h_{ij} \quad (5)$$

Where H_j^D is the destination-based total exposure to the destination j.

3.5.2. Mean transit heat exposure index (Mean THEI)

Total THEI or total exposure is a function of three factors: 1) the feels-like temperature at the waiting stops and the street links, 2) the average travel time, and 3) the number of trips originated to/from a given location. In other words, with more ridership or demand between

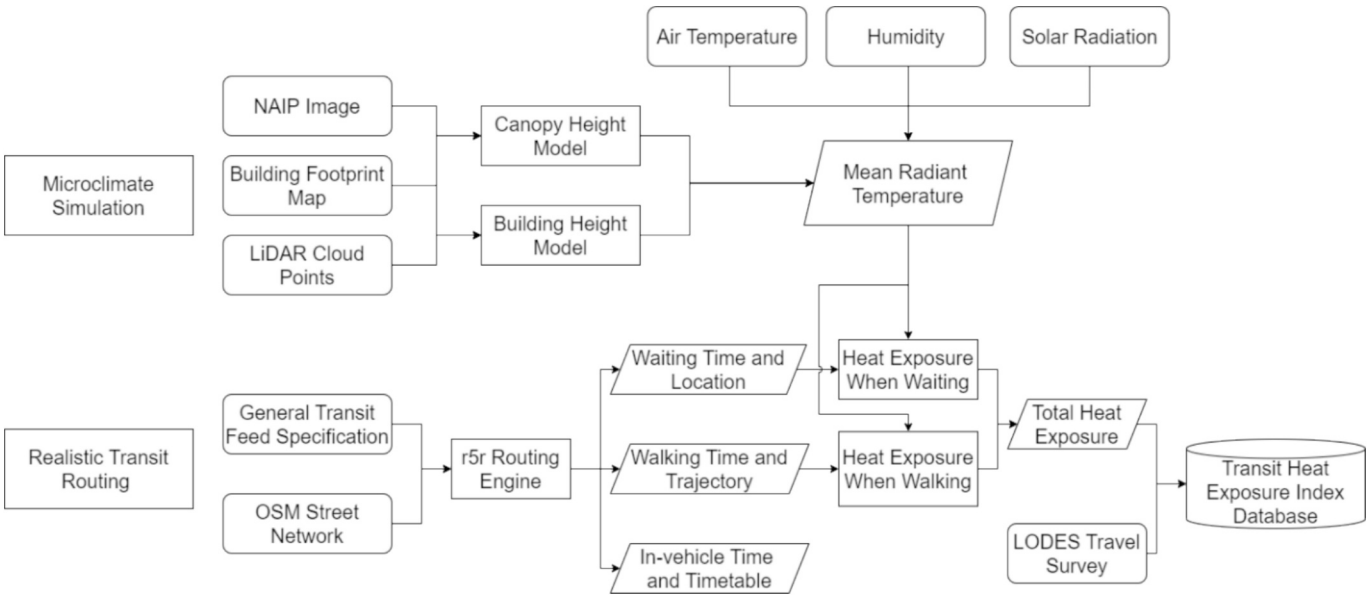

Fig. 2. A diagram showing the methodological structure of THEI.

the OD pair, the total exposure will increase. Therefore, to gauge transit-based heat exposure with a temperature-esque measure, we introduce the *mean THEI*. It is a measure of average level of heat exposure experienced by transit riders during their transit trip experience. It is defined as:

$$e = \frac{H}{t} = \frac{\sum w_{ij} \cdot h_{ij}}{\sum t_{ij}} \tag{6}$$

Where: H is the total THEI, which could be aggregated to the origins, destinations, or networks. t is the total travel time, which is calculated as the sum of all trips, including the walking, waiting, and in-vehicle time. Note that the unit of e is Celsius, the same as temperature. The measure represents the heat that public transit users experienced in a single unit amount of time, which is independent of the number of trips made.

Similar to the total exposure, mean THEI can also be calculated for the entire transit systems or using the origin-base and destination-based versions of the measure.

3.5.3. Heat exposure composition from walking and waiting

It is largely unknown from prior studies whether walking or waiting is responsible for most of the heat and the specific composition of the heat generated from the two processes. A major advantage of the method introduced in this paper is the ability to produce high-resolution heat exposure measures at a very detailed level for each segment of a trip, which allows one to decompose the total heat exposure due to exposure during walking and waiting times. The share of heat from walking time can be calculated as:

$$r = \frac{H^w}{H^t + H^w} \tag{7}$$

Where r is the share of heat exposure from walking, H^t is the total THEI from waiting, and H^w is the total THEI from walking.

3.5.4. Network-based heat exposure

The network-based THEI metric measures the contribution of each road link and bus stop to total heat exposure by considering the time spent by the total number of users that traverse each road or wait at each stop. The contribution of each road link and stop to total heat exposure is defined as

$$H_k^T = \sum_{ij} w_{ij} \cdot h_{ijk} \tag{8}$$

Where: H_k^T is the exposure contribution of a road or a stop T, and h_{ijk} is the heat exposure experienced at the road/stop k by a user travelling from census block i to census block j. In practice, we calculated three measures: 1) total exposure of each road when walking, which measures the heat contribution of the road to all users' heat exposure, 2) total exposure for each bus stop when waiting, which measures the heat contribution of the bus stop to all users' heat exposure, and 3) the sum of the two exposures aggregated their corresponding census block group. We used the spatial join function with largest overlap operation in the ArcGIS Pro to calculate the third measure, which means if a street link crosses two census block groups, we will be aggregating its heat to the census block group with which it has the largest overlap.

4. Results

4.1. Spatiotemporal pattern of THEI

Fig. 3 visualizes the total exposure in each census block group for Miami in quantile classification. In general, the accumulated heat exposure to heat of transit passengers travelling to and from neighborhoods in the suburban areas was rather low. This is largely because there were very few transit trips to and from these neighborhoods due to low transit connectivity. However, it is also noteworthy that the core of the downtown also presented lower total exposure which generally has higher local feels-like temperature and higher amounts of public transit trips and higher accessibility.

This counter-intuitive results arise because THEI considers human mobility behavior when calculating heat. Total THEI is dependent on three components: potential exposure time, temperature values, and number of trips. While the downtown is generally a heat island with higher local temperature, it usually has more frequent transit services and higher density, which makes the residents there wait less and walk less. Meanwhile, the weight, i.e., commute flow, is also higher in downtown. Therefore, the number of trips, feels-like temperature, and exposure time can have heterogenous effect on the outcomes: higher feels-like temperature, higher number of trips, and higher exposure time can all contribute to a higher total exposure.

Meanwhile, Fig. 3 shows the resemblance between the origin-based and destination-based measures. It can be because unconnected areas generally have lower access to and from other places, and most public transit routes are symmetrical, which means the trips back and forth

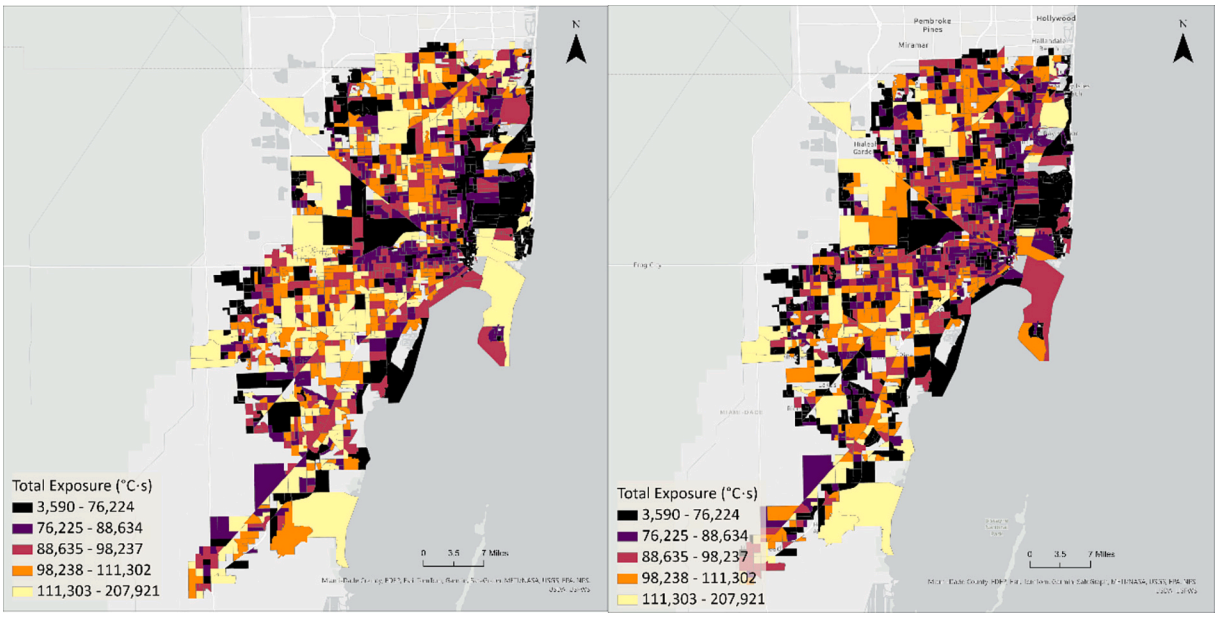

Fig. 3. Total THEI of every census block group in Miami. Left: aggregated by origin; right: aggregated by destination. Maps are generated per the origin-based layer's quantile classification.

generally have similar travel time and geometries.

4.1.1. Mean THEI

In contrast to total THEI, the mean THEI is primarily determined by feels-like temperature and exposure time. To investigate the patterns of the average heat exposure, we further visualized the mean THEI in Fig. 4. The mean transit heat exposure in Miami downtown core was significantly lower than their urban outskirts and suburbs. This means that the average experienced heat in a unit amount of time when a resident is accessing other opportunities via public transit is lower in the downtown core. The downtown areas generally have higher level of transit infrastructure and sidewalk infrastructure, which reduces walking, waiting, and transfer time (L. Liu and Miller, 2020; Wang and Cao, 2017). For example, the exposure from walking in downtown tends to be much lower since downtowns have much higher density, more high-level buildings and tree canopies, and more extensive sidewalk network (X. Li, 2021; L. Liu et al., 2023). Moreover, the exposure during waiting would also tend to be lower due to higher frequency for transit routes in downtown area.

Meanwhile, like the total exposure, the origin-base and destination-based measures are highly similar for the same reasons stated above. There could be factors that contribute to the minor differences, such as differences in transit geometry and travel time and asymmetrical commute flow from and to the location.

4.2. Source of heat exposure

Fig. 5 visualizes the heat exposure from walking and waiting,

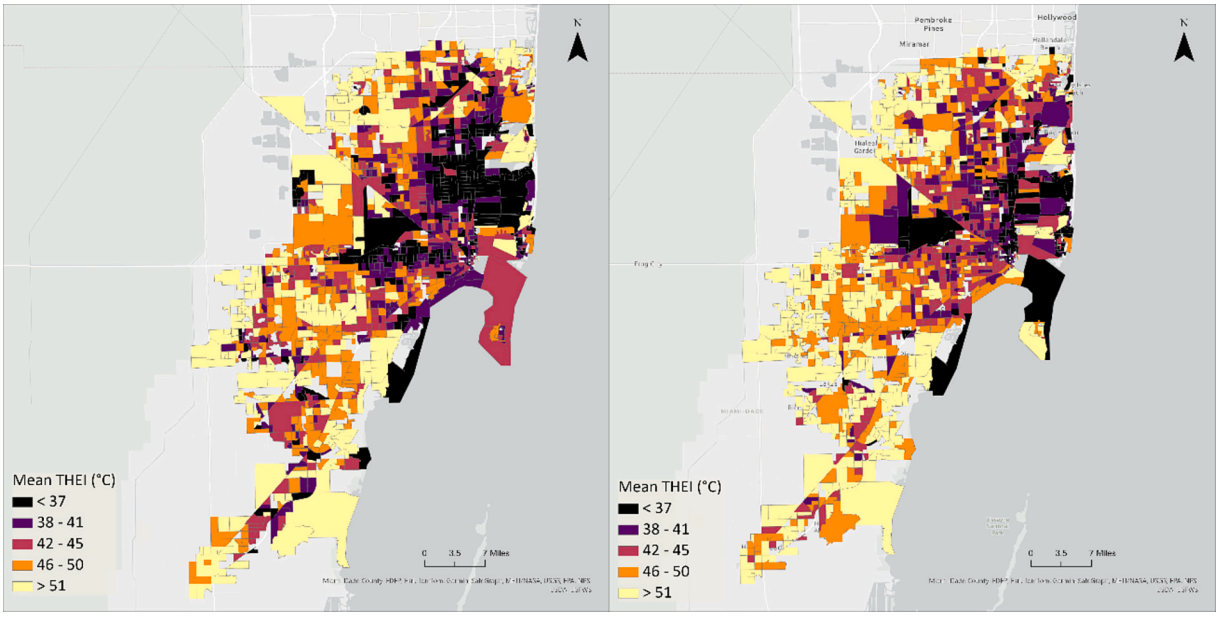

Fig. 4. Mean THEI of every census block group in Miami. Left: aggregated by origin; right: aggregated by destination. Maps are generated per the origin-based layer's quantile classification.

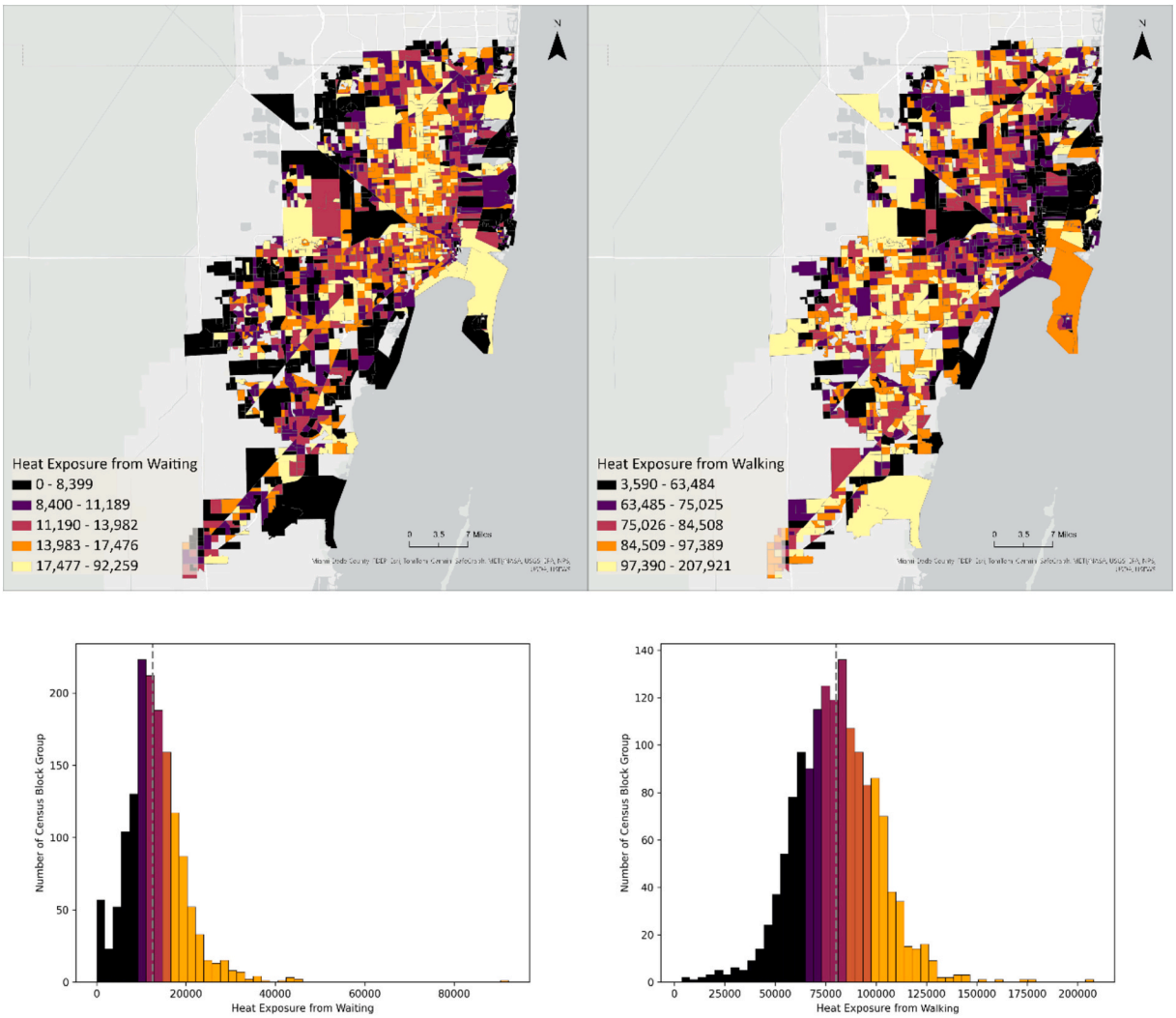

Fig. 5. Heat exposure from walking and waiting. Map symbols are generated with quantile classification.

respectively. Note that we aggregated the heat to their origin, meaning that the measures represent the heat experience of local residents when accessing other opportunities. First, between walking and waiting, walking accounts for most of the heat exposure in Miami. Fig. 6 also visualizes the share of exposure from walking out of the total heat exposure. This confirms that walking is the main source of heat exposure in Miami with a global average of 86 %, meaning that 86 % of heat exposure is from walking during first mile, last mile, and transfers, and only 14 % of heat exposure is from waiting at bus stops. In a practical sense, this provides firsthand evidence that future interventions should prioritize improving the walking experience of public transit passengers, despite being a functional but not an intrinsic part of the public transit system and outside transit authorities' responsibility. Second, Fig. 5 also visualizes the histogram of the two maps, and the two values have very different patterns. Interestingly, heat exposure from walking follows a normal distribution, while heat exposure from waiting follows a log-normal distribution.

Fig. 7 visualizes the heat contribution of each street link and bus stop. Only a very small number of street links contributed to the total heat exposure. Out of 1,066,000 street links, only 98,879 street links generated heat exposure. Meanwhile, the distribution of heat contribution is highly uneven. The top 5000 street segments generating heat exposure, which is 5 % of street links with nonzero heat generation and less than 0.5 % of all street links, account for 60 % of the heat exposure generation on roads. This means that authorities can concentrate intervention efforts on a small number of road links in the sidewalk network, such as adding tree canopies and sidewalk shelters, to reduce the heat exposure of most of the transit riders. As an example, the mere top 100 street segments, whose length is only 16 km in total, account for almost 10 % of the heat exposure. This finding provides actionable information for the authorities to address the heat issue in a very practical, efficient, and cost-effective manner.

Meanwhile, the heat exposure at bus stops is not negligible. Among the 8164 bus stops, only at 3987 bus stops (less than half) have riders exposed to heat, and the top 400 bus stops (top 5 %) account for 67 % of the total heat exposure at bus stops. This resonates well with and complements our findings above that targeted interventions could substantially reduce the heat exposure of transit passengers at very low costs. In fact, due to the nature of bus stops, it is significantly easier to install shelters at the bus stops than on the sidewalks, in terms of both labor and economics, to reduce transit users' exposure to heat. And the installation of bus shelters is also positively associated with other factors such as increased ridership, safety, and revenue (Ewing, 2000; Kim et al., 2020).

Fig. 8 further combines the two sources of heat together and aggregates them to each census block group. As a star-shape public transit system, which heavily depends on transfers near the downtown, it is intuitive and natural to observe that most of the generated heat is from the heart of the city. Meanwhile, it is also interesting that the high-heat-contribution areas can also have much lower mean THEI for local residents (origin-based) and lower mean THEI for other travelers to there

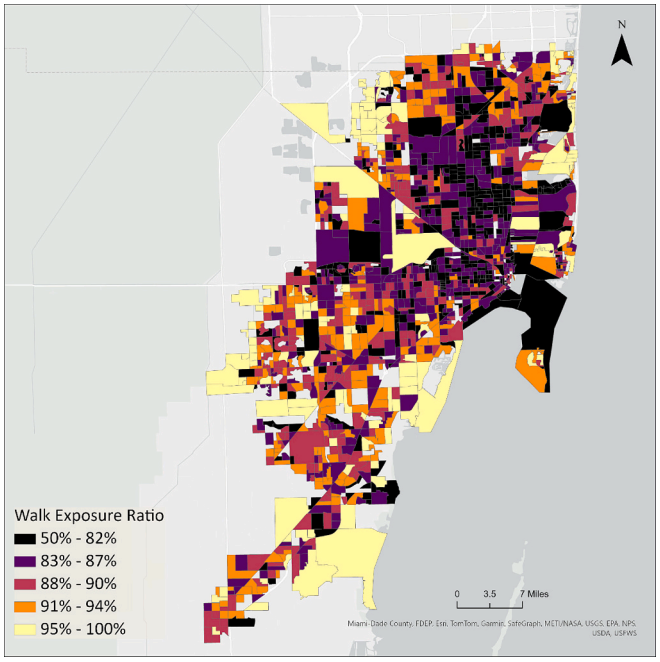

Fig. 6. Proportion of exposure due to walking. Maps are generated with quantile classification.

(destination-based), which means the areas that contribute the most to the heat can have a much lower experienced heat exposure for local residents. This also resonates well with the discrepancy between MRT and THEI measures.

5. Discussion

Our spatiotemporal analyses in Miami offer multiple practical insights, which would make potential impacts on future research and planning works. We discuss how the application of THEI can inform strategies to enhance transit systems' heat resilience in three aspects:

5.1. Immediate adaptation

Our results show that there are multiple adjustments that transit systems can enact to immediately remedy the heat exposure of the transit users. First, there is an urgent need to adopt a *behavior-centric* or *people-centric approach* to measure people's heat exposure experience (Miller, 2005; Park and Kwan, 2017). Although traditional *place-centric* measures, i.e., measuring the heat experience of users by their home/local temperature, have been proven to be useful, these place-based measures may not be an accurate representation of people's heat experience, as shown in Fig. 9. Note that this insight applies to all people (Karner et al., 2015), although it may be more pronounced among public transit riders. For example, a drivers' perceived heat exposure would not

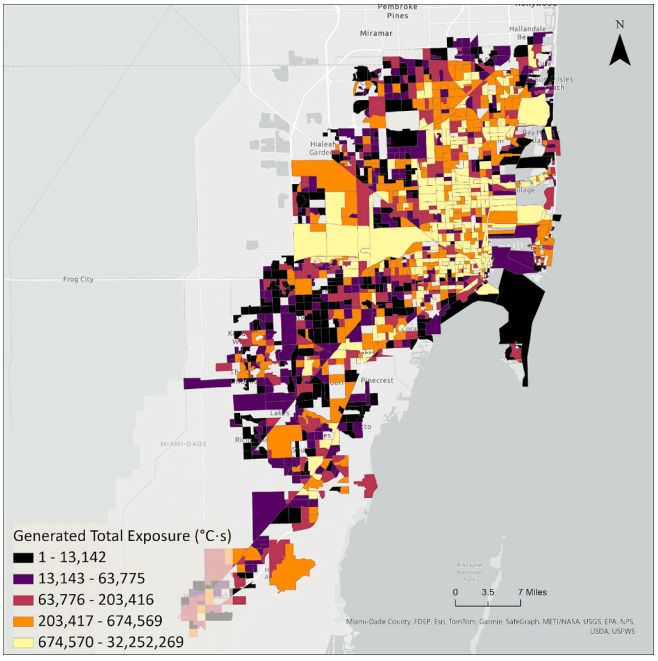

Fig. 8. Generated total exposure for each census block group. Symbols are generated with quantile classification.

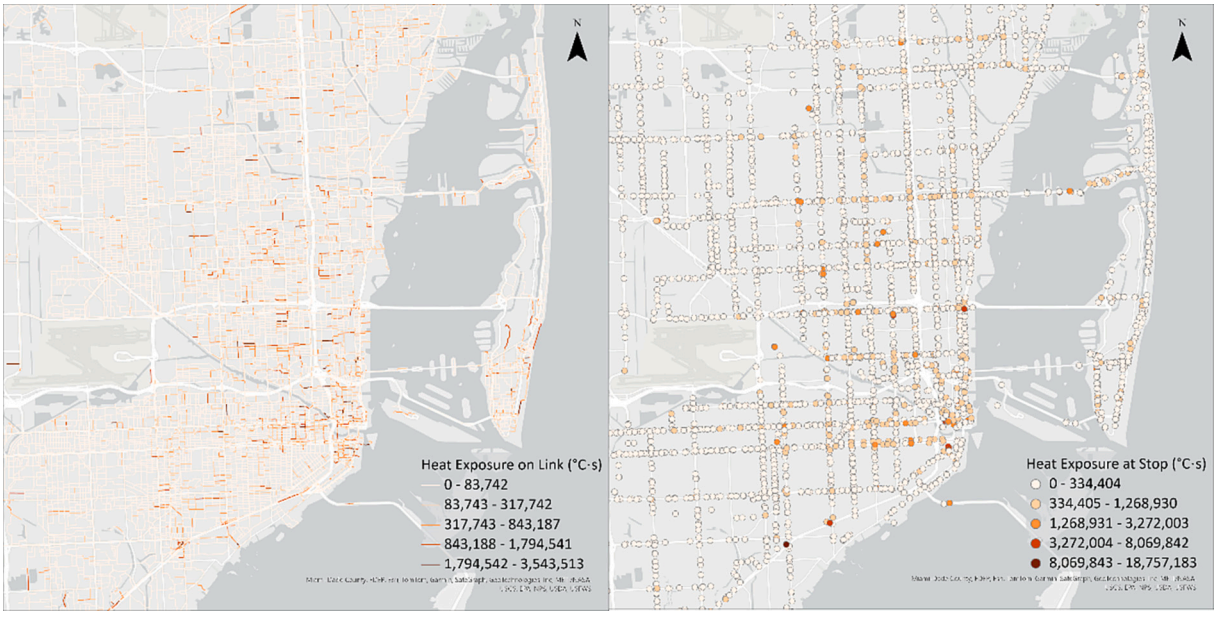

Fig. 7. Heat exposure on road links and bus stops. Maps are generated with natural break Jenks classification.

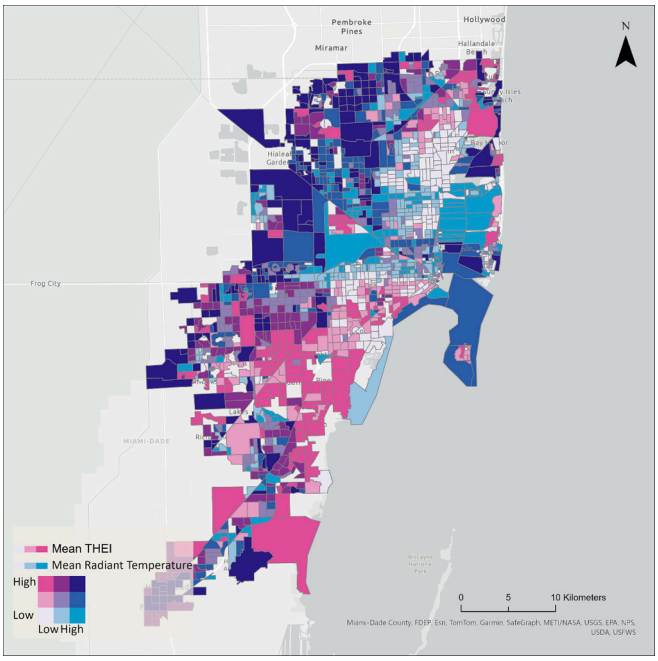

Fig. 9. Bivariate map of Miami's mean THEI (mobility-based heat exposure) and mean radiant temperature (local heat exposure). Map symbols are generated with 3*3 quantile classification.

be their local heat situation around their home, but rather more about the heat near their destination or parking. To achieve this goal, we need a coordinated endeavor to integrate the existing research on travel behavior research and city planning.

The introduction of THEI also creates new opportunities to adjust bus timetables via optimization methods to reduce heat exposure during future interventions. Meanwhile, the case study shows that walking is the primary source of transit heat exposure in Miami-Dade County, which suggests local governments should prioritize reducing walking exposure during future intervention. In other words, solving the first-mile and last-mile problem is still the priority of future transit planning, particularly in the context of combating heat exposure. However, very few papers discussed the optimization of transit systems based on heat exposure, which could be a potential topic for future research.

5.2. Long-term preparedness

With high-frequency transit service, connected walking infrastructure, and well-optimized timetable, Miami downtown has much lower exposure than other suburbs and nearby urban outskirts, despite having similar or even higher local feels-like temperature. This conclusion can be seemingly contradicting with prior studies that use traditional static measures (Deilami et al., 2018; Nwakaire et al., 2020), but it is consistent with the finding in a recent behavior-based exposure study (Ahmed et al., 2024). Therefore, transport infrastructure plays a greater role than environmental conditions, allowing us to strategically enhance the built environment to strengthen system resilience.

Furthermore, a very small percentage of road links and bus stops contribute to most heat exposure for all public transit users. This finding points out a practical and efficient solution to the heat exposure problem: it suggests that targeted interventions to create shades via tree planting or shelter building on very few critical street links and bus stops would be sufficient to reduce heat exposure for many people across a broad area.

Similarly, our results also provide evidence for future stop-level infrastructure building. Although heat exposure during waiting times at bus stops is not the dominating factor, building bus shelters and planting trees at targeted bus stops could be a much easier and more effective intervention, whose effectiveness have been extensively discussed by prior studies (Dzyuban et al., 2021; Lanza and Durand, 2021). For example, some recent thermal technological progress, such as natural cooling stations, can be enacted at bus stops but not on road links. This can decrease the feels-like temperature at the stops to a lower level than on the roads, providing more potentials for heat reduction (Medina et al., 2022; Mokhtari et al., 2022). Meanwhile, as road work and improvement are usually out of the jurisdiction of public transit authorities, the intervention on the bus stop level is also more practical from a political and legal standpoint.

5.3. Social impacts

Extreme heat disproportionately affects vulnerable populations, including low-income communities and transit-dependent individuals. The proposed THEI serves as a valuable tool for assessing the social impacts of extreme heat on communities and population groups, providing innovative and practical insights to guide transit heat resilience strategies. For example, our Miami case study reveals that transit-dependent communities who rely on low-frequency bus services experience disproportionately higher heat exposure, particularly in the urban outskirts. Transit agencies can address this disparity by increasing the service frequency or adjusting the timetable. People older than 55 years old are especially vulnerable to extreme heat and long-time travel. However, Western Miami (Kendall), which has a higher percentage of senior residents, has higher average heat exposure during transit trips. Likewise, some areas with more people with disabilities also have higher exposure, which can exacerbate inequalities. Meanwhile, transit-related heat exposure for city residents may not necessarily be higher in areas marked by urban heat island effect. This challenges the common assumption that urban centers inherently experience greater heat exposure. Instead, cities can overcome the natural environmental disadvantages for transit-dependent communities by resilience planning and long-term infrastructure improvements, as we systematically discussed above.

There are multiple topics that future studies can further address. Future research can use the THEI system to minimize heat exposure in a city or for a public transit system. While it is hard to control the temperature, it is within the power of transit planners and transit authorities to conduct system redesign to reduce exposure time. Future research could also explore strategies for positioning tree canopies or bus stops to help lower temperatures.

A major limitation of the method is that the meteorological parameters in the SOLWEIG model are constant for the whole city due to the lack of higher-resolution data, and the temporal resolution of the meteorological data is 30 min. Future studies should use meteorological data with higher resolutions if possible. Future studies could also try to incorporate other factors that can contribute to heat exposure in transit trips, such as how thermal comfort might be affected by vehicle crowding and terrain elevation. Meanwhile, while we have provided some discussions on the contributing factors of transit heat exposure index, we believe that future studies should expand the analysis of heat sources and discuss the heterogeneous implications for different demographic groups. Future studies should also explore different interventions, such as strategic tree planting at high-volume street links, to reduce heat exposure and address heat-related concerns in transportation equity.

The method employed in this study first determines the fastest trip itinerary between a given OD pair and subsequently calculates heat exposure. Future research could try to incorporate heat exposure while walking along street links into the routing algorithm to reflect how some pedestrians choose their trip itineraries trying to travel time and heat exposure costs. Finally, the paper used the annual LODES survey in 2021 to weigh the 2023 heat exposure data because the most recent LODES data in 2023 are still unavailable, which can reduce the accuracy of our

empirical results and harm the generalizability of these findings. Future studies can use data from the same year and more accurate or higher-resolution ridership data as weights to enhance the robustness of study findings. In addition, while the method proposed here provides a replicable and scalable model that can be applied in different cities or contexts for transit heat exposure measurement, the THEI index can be further validated and refined through on-the-ground data collection efforts such as personal monitoring with mobile sensors.

6. Conclusion

This study introduces the Transit Heat Exposure Index (THEI), a novel and comprehensive method for measuring heat exposure experienced by public transit riders. By integrating high-resolution microclimate simulation and transit routing techniques, our approach captures detailed feels-like temperatures and travel times to provide an accurate assessment of heat exposure in a complex urban environment. The empirical results in Miami, Florida, show that despite the urban heat island effect causing higher temperatures, better transit access reduces overall heat exposure in downtown Miami. Walking, rather than waiting, is the primary source of heat exposure, showing the importance of pedestrian infrastructure in mitigating heat risk. Additionally, a small number of streets and bus stops contribute disproportionately to transit heat exposure, highlighting opportunities for targeted interventions.

This method fills a major knowledge gap by providing spatially detailed data on heat exposure, enabling urban planners and policymakers to design more heat-resilient transit systems. By identifying high-exposure zones and understanding the primary sources of heat, future strategies can focus on improving shade coverage, tree canopy, and transit access. The findings from this study offer a new approach for reducing heat exposure in public transit, improving thermal comfort, and enhancing equity for vulnerable populations who rely on transit services.

CRediT authorship contribution statement

Luyu Liu: Writing – original draft, Validation, Methodology, Funding acquisition, Software, Investigation, Formal analysis, Conceptualization, Writing – review & editing, Visualization, Data curation. **Xiaojiang Li:** Writing – review & editing, Validation, Formal analysis, Methodology, Data curation, Visualization. **Rafael H.M. Pereira:** Validation, Writing – review & editing, Software. **Xiang Yan:** Supervision, Conceptualization, Validation, Investigation, Writing – review & editing.

Funding source

We gratefully acknowledge funding support from the Center for Equitable Transit-Oriented Communities Tier-1 University Transportation Center (Grant No. 69A3552348337). This work was also supported by the National Science of Foundation No. 2525118.

Declaration of competing interest

The authors have no financial and personal relationships with other people or organizations that could inappropriately influence the work.

Data availability

Data will be made available on request.

References

Ahmed, N., Lee, J., Liu, L., Kim, J., Jang, K.M., Wang, J., 2024. The cost of climate change: A generalized cost function approach for incorporating extreme weather exposure into public transit accessibility. Comput. Environ. Urban. Syst. 112, 102145.

Arbex, R., Cunha, C.B., 2020. Estimating the influence of crowding and travel time variability on accessibility to jobs in a large public transport network using smart card big data. J. Transp. Geogr. 85, 102671.

Chen, Y., Yang, J., Yu, W., Ren, J., Xiao, X., Xia, J.C., 2023. Relationship between urban spatial form and seasonal land surface temperature under different grid scales. Sustain. Cities Soc. 89, 104374.

Cheung, P.K., 2018. Comparing the cooling effects of a tree and a concrete shelter using PET and UTCI. Build. Environ. 130, 49–61.

Crowley, K., 2023, September 13. Miami Playground Surface Hits 177.9 Degrees Amid Record-Breaking Heat in Florida. USA TODAY. https://www.usatoday.com/story/news/weather/2023/08/11/miami-playground-measures-178-degrees-hot-surfaces/70574217007/.

Curriero, F.C., Heiner, K.S., Samet, J.M., Zeger, S.L., Strug, L., Patz, J.A., 2002. Temperature and mortality in 11 cities of the eastern United States. Am. J. Epidemiol. 155 (1), 80–87.

Deilami, K., Kamruzzaman, M., Liu, Y., 2018. Urban heat island effect: A systematic review of spatio-temporal factors, data, methods, and mitigation measures. Int. J. Appl. Earth Obs. Geoinf. 67, 30–42.

Deschenes, O., 2014. Temperature, human health, and adaptation: A review of the empirical literature. Energy Econ. 46, 606–619.

Developers, Google, 2020. GTFS Static Overview | Static Transit | Google Developers. https://developers.google.com/transit/gtfs/.

Dong, J., Peng, J., He, X., Corcoran, J., Qiu, S., Wang, X., 2020. Heatwave-induced human health risk assessment in megacities based on heat stress-social vulnerability-human exposure framework. Landsc. Urban Plan. 203, 103907.

Dzyuban, Y., Hondula, D.M., Coseo, P.J., Redman, C.L., 2021. Public transit infrastructure and heat perceptions in hot and dry climates. Int. J. Biometeorol. 1–12.

Ewing, R., 2000. Asking transit users about transit-oriented design. Transp. Res. Rec. 1735 (1), 19–24.

Fan, H., Lu, H., Lyu, G., Guin, A., Guensler, R., 2024. A Framework for Assessing Cumulative Exposure to Extreme Temperatures During Transit Trip (No. arXiv:2408.04081). arXiv. http://arxiv.org/abs/2408.04081.

Fraser, A.M., Chester, M.V., 2017. Transit system design and vulnerability of riders to heat. J. Transp. Health 4, 216–225.

Fraser, A.M., Chester, M.V., Eisenman, D., Hondula, D.M., Pincetl, S.S., English, P., Bondank, E., 2017. Household accessibility to heat refuges: residential air conditioning, public cooled space, and walkability. Environ. Plan. B 44 (6), 1036–1055.

Geofabrik, 2023. Geofabrik Download Server. https://download.geofabrik.de/.

Gu, X., Chen, P., Fan, C., 2024. Socio-demographic inequalities in the impacts of extreme temperatures on population mobility. J. Transp. Geogr. 114, 103755.

Hsu, A., Sheriff, G., Chakraborty, T., Manya, D., 2021. Disproportionate exposure to urban heat island intensity across major US cities. Nat. Commun. 12 (1), 2721.

Hu, J., Zhou, Y., Yang, Y., Chen, G., Chen, W., Hejazi, M., 2023. Multi-city assessments of human exposure to extreme heat during heat waves in the United States. Remote Sens. Environ. 295, 113700.

Huang, X., Jiang, Y., Mostafavi, A., 2024. The emergence of urban heat traps and human mobility in 20 US cities. npj Urban Sustain. 4 (1), 6.

Iseki, H., Tingstrom, M., 2014. A new approach for bikeshed analysis with consideration of topography, street connectivity, and energy consumption. Comput. Environ. Urban. Syst. 48, 166–177.

Karner, A., Hondula, D.M., Vanos, J.K., 2015. Heat exposure during non-motorized travel: implications for transportation policy under climate change. J. Transp. Health 2 (4), 451–459.

Keellings, D., Waylen, P., 2014. Increased risk of heat waves in Florida: characterizing changes in bivariate heat wave risk using extreme value analysis. Appl. Geogr. 46, 90–97.

Kim, J.Y., Bartholomew, K., Ewing, R., 2020. Another one rides the bus? The connections between bus stop amenities, bus ridership, and ADA paratransit demand. Transp. Res. A Policy Pract. 135, 280–288.

Klein, T., Anderegg, W.R., 2021. A vast increase in heat exposure in the 21st century is driven by global warming and urban population growth. Sustain. Cities Soc. 73, 103098.

Kuras, E.R., Hondula, D., Brown-Saracino, J., 2015. Heterogeneity in individually experienced temperatures (IETs) within an urban neighborhood: insights from a new approach to measuring heat exposure. Int. J. Biometeorol. 59, 1363–1372.

Kuras, E.R., Richardson, M.B., Calkins, M.M., Ebi, K.L., Hess, J.J., Kintziger, K.W., Jagger, M.A., Middel, A., Scott, A.A., Spector, J.T., 2017. Opportunities and challenges for personal heat exposure research. Environ. Health Perspect. 125 (8), 085001.

Lanza, K., Durand, C.P., 2021. Heat-moderating effects of bus stop shelters and tree shade on public transport ridership. Int. J. Environ. Res. Public Health 18 (2), 463.

Li, X., 2021. Investigating the spatial distribution of resident's outdoor heat exposure across neighborhoods of Philadelphia, Pennsylvania using urban microclimate modeling. Sustain. Cities Soc. 72, 103066.

Li, X., Wang, G., 2021a. Examining runner's outdoor heat exposure using urban microclimate modeling and GPS trajectory mining. Comput. Environ. Urban. Syst. 89, 101678.

Li, X., Wang, G., 2021b. GPU parallel computing for mapping urban outdoor heat exposure. Theor. Appl. Climatol. 145 (3–4), 1101–1111. https://doi.org/10.1007/s00704-021-03692-z.

Li, R., Chester, M.V., Hondula, D.M., Middel, A., Vanos, J.K., Watkins, L., 2023. Repurposing mesoscale traffic models for insights into traveler heat exposure. Transp Res Part D: Transp Environ 114, 103548.

Liu, L., Miller, H.J., 2020. Measuring risk of missing transfers in public transit systems using high-resolution schedule and real-time bus location data. Urban Stud. 58 (15), 3140–3156.
Liu, L., Porr, A., Miller, H.J., 2022. Realizable accessibility: evaluating the reliability of public transit accessibility using high-resolution real-time data. J. Geogr. Syst. 1–23.
Liu, L., Kar, A., Tokey, A.I., Le, H.T., Miller, H.J., 2023. Disparities in public transit accessibility and usage by people with mobility disabilities: an evaluation using high-resolution transit data. J. Transp. Geogr. 109, 103589.
Liu, Y., Chu, C., Zhang, R., Chen, S., Xu, C., Zhao, D., Meng, C., Ju, M., Cao, Z., 2024. Impacts of high-albedo urban surfaces on outdoor thermal environment across morphological contexts: A case of Tianjin, China. Sustain. Cities Soc. 100, 105038.
Lu, Y., Yue, W., Liu, Y., Huang, Y., 2021. Investigating the spatiotemporal non-stationary relationships between urban spatial form and land surface temperature: A case study of Wuhan, China. Sustain. Cities Soc. 72, 103070.
Mayer, H., Höppe, P., 1987. Thermal comfort of man in different urban environments. Theor. Appl. Climatol. 38 (1), 43–49. https://doi.org/10.1007/BF00866252.
McAllister, C., Stephens, A., Milrad, S.M., 2022. The heat is on: observations and trends of heat stress metrics during Florida summers. J. Appl. Meteorol. Climatol. 61 (3), 277–296.
Medina, D.C., Delgado, Mc, G., Amores, T. R. P., Toulou, A., Ramos, J. S., & Domínguez, S. Á., 2022. Climatic control of urban spaces using natural cooling techniques to achieve outdoor thermal comfort. Sustainability 14 (21), 14173.
Microsoft., 2024. GitHub—Microsoft/USBuildingFootprints [Computer software]. Microsoft. https://github.com/microsoft/USBuildingFootprints (Original work published 2018).
Miller, H.J., 2005. Place-based versus people-based accessibility. In: Access to Destinations. Emerald Group Publishing Limited, pp. 63–89 https://www.emerald.com/insight/content/doi/10.1108/9780080460550-004/full/html.
Mokhtari, R., Ulpiani, G., Ghasempour, R., 2022. The Cooling Station: combining hydronic radiant cooling and daytime radiative cooling for urban shelters. Appl. Therm. Eng. 211, 118493.
National Agriculture Imagery Program, 2023. National Agriculture Imagery Program—NAIP Hub Site. https://naip-usdaonline.hub.arcgis.com/.
Nazarian, N., Lee, J.K., 2021. Personal assessment of urban heat exposure: A systematic review. Environ. Res. Lett. 16 (3), 033005.
NREL, 2024. NSRDB: National Solar Radiation Database. https://nsrdb.nrel.gov/.
Nwakaire, C.M., Onn, C.C., Yap, S.P., Yuen, C.W., Onodagu, P.D., 2020. Urban Heat Island studies with emphasis on urban pavements: A review. Sustain. Cities Soc. 63, 102476.
OpenMobilityData, 2023. OpenMobilityData—Public Transit Feeds From Around the World. https://transitfeeds.com/.
Park, Y.M., Kwan, M.-P., 2017. Individual exposure estimates may be erroneous when spatiotemporal variability of air pollution and human mobility are ignored. Health Place 43, 85–94.
Pereira, R.H.M., Saraiva, M., Herszenhut, D., Braga, C.K.V., Conway, M.W., 2021. r5r: rapid realistic routing on multimodal transport networks with r 5 in r. Findings 21262.
Romaszko, J., Dragańska, E., Jalali, R., Cymes, I., Glińska-Lewczuk, K., 2022. Universal climate thermal index as a prognostic tool in medical science in the context of climate change: A systematic review. Sci. Total Environ. 828, 154492.
Saaroni, H., Ben-Dor, E., Bitan, A., Potchter, O., 2000. Spatial distribution and microscale characteristics of the urban heat island in Tel-Aviv, Israel. Landsc. Urban Plan. 48 (1–2), 1–18.
U.S Geological Survey, 2023. Lidar Point Cloud—USGS National Map 3DEP Downloadable Data Collection | USGS Science Data Catalog. https://data.usgs.gov/datacatalog/data/USGS:b7e353d2-325f-4fc6-8d95-01254705638a.
US Census Bureau, 2020. 2016-2020 American Community Survey 5-Year Estimates. https://data.census.gov/table.
US Census Bureau Center for Economic Studies, 2023. Longitudinal Employer-Household Dynamics. https://lehd.ces.census.gov/data/.
Vanos, J.K., Rykaczewski, K., Middel, A., Vecellio, D.J., Brown, R.D., Gillespie, T.J., 2021. Improved methods for estimating mean radiant temperature in hot and sunny outdoor settings. Int. J. Biometeorol. 65 (6), 967–983.
Wang, J., Cao, X., 2017. Exploring built environment correlates of walking distance of transit egress in the Twin Cities. J. Transp. Geogr. 64, 132–138.
Wong, K.V., Paddon, A., Jimenez, A., 2013. Review of world urban heat islands: many linked to increased mortality. J. Energy Resour. Technol. 135 (2), 022101.
World Weather Online, 2024. World Weather Online. WorldWeatherOnline.Com. https://www.worldweatheronline.com/.
Yau, Y., Chew, B., 2014. A review on predicted mean vote and adaptive thermal comfort models. Build. Serv. Eng. Res. Technol. 35 (1), 23–35.
Yin, Z., Liu, Z., Liu, X., Zheng, W., Yin, L., 2023. Urban heat islands and their effects on thermal comfort in the US: New York and New Jersey. Ecol. Indic. 154, 110765.
Zhang, H., Zhao, X., Kang, M., Han, J., 2022. Contrasting changes in fine-scale land use structure and summertime thermal environment in downtown Shanghai. Sustain. Cities Soc. 83, 103965.